Articles

Off-Resonance Rotating Frame Spin–Lattice NMR Relaxation Studies of Phosphorus Metabolite Rotational Diffusion in Bovine Lens Homogenates†

G. Herbert Caines,‡ Thomas Schleich,*,‡ Courtney F. Morgan,‡,§ and Patricia N. Farnsworth‖

Department of Chemistry, University of California, Santa Cruz, California 95064, and Department of Physiology, University of Medicine and Dentistry—New Jersey Medical School, Newark, New Jersey 07103

Received January 24, 1990; Revised Manuscript Received May 2, 1990

ABSTRACT: The rotational diffusion behavior of phosphorus metabolites present in calf lens cortical and nuclear homogenates was investigated by the NMR technique of ^{31}P off-resonance rotating frame spin–lattice relaxation as a means of assessing the occurrence and extent of phosphorus metabolite–lens protein interactions. ^{31}P NMR spectra of calf lens homogenates were obtained at 10 and 18 °C (below and above the cold cataract phase transition temperature, respectively) at 7.05 T. Effective rotational correlation times ($\tau_{0,eff}$) for the major phosphorus metabolites present in cortical and nuclear bovine calf lens homogenates were derived from nonlinear least-squares analysis of R vs ω_e (spectral intensity ratio vs precessional frequency about the effective field) data with the assumption of isotropic reorientational motion. Intramolecular dipole–dipole (^1H–^{31}P, ^{31}P–^{31}P), chemical shift anisotropy (CSA), and solvent (water) translational intermolecular dipole–dipole (^1H–^{31}P) relaxation contributions were assumed in the analyses. In those cases where the limiting value of the spectral intensity ratio failed to reach unity at large offset frequency, a modified formalism incorporating chemical exchange mediated saturation transfer between two sites was used. Values of $\tau_{0,eff}$ for phosphorus metabolites present in the cortex varied from a low of ca. 2 ns [L-α-glycerophosphocholine (GPC)] to a high of 12 ns (α-ATP) at 10 °C, whereas at 18 °C the range was from ca. 1 to 9 ns. For the nucleus the $\tau_{0,eff}$ values ranged from ca. 3 ns (GPC) to 41 ns (P_i) at 10 °C; at 18 °C the corresponding values ranged from 4 to 39 ns. For PME (phosphomonoester; in lens the predominant metabolite is L-α-glycerol phosphate) at 18 °C evidence was obtained for binding and subsequent exchange with solidlike protein domains. The diversity in $\tau_{0,eff}$ values for lenticular phosphorus metabolites is suggestive of differential binding to more slowly tumbling macromolecular species, most likely lens crystallin proteins. Corresponding measurement of $\tau_{0,eff}$ values for the mobile protein fraction present in calf lens cortical and nuclear homogenates at 10 and 18 °C, by ^{13}C off-resonance rotating frame spin–lattice relaxation, provided average macromolecular correlation times that were assumed to represent the bound metabolite state. A fast-exchange model (on the T_1 time scale), between free and bound forms, was employed in the analysis of the metabolite R vs ω_e curves to yield the fraction of free (unbound) metabolite (Θ_{free}). The following Θ_{free} values for phosphorus metabolite in calf lens homogenates were obtained at 10 and 18 °C, respectively: (cortex) GPC, 0.98, 0.98; PME, 0.97, 0.92; P_i, 0.99, 0.99; ATP, 0.75, 0.85; (nucleus) GPC, 0.98, 0.96; PME, 0.80, 0.63; P_i, 0.84, 0.87. The results of this study establish the occurrence of significant temperature-dependent (above and below the cold cataract phase transition temperature) binding of ATP (cortex) and PME (nucleus) and P_i (nucleus) in calf lens.

Anaerobic glycolysis is the major source of metabolic energy for the maintenance of eye lens function (Cheng & Chylack, 1985), and thus the regulation of this pathway assumes considerable importance. An understanding of the glycolytic pathway regulatory process requires, in part, knowledge of the availability, utilization, and generation of phosphorus metabolites in lenticular metbolic processes (Farnsworth et al., 1989). Standard biochemical assays (Harding & Crabbe, 1984; Cheng & Chylack, 1985) and noninvasive ^{31}P nuclear magnetic resonance (NMR)[1] spectroscopic techniques (Greiner et al., 1981, 1982, 1985; Gonzalez et al., 1984; Willis & Schleich, 1986; Williams et al., 1988) have been employed to assess the identity and concentration of lens phosphorus metabolites. These studies indicate that there is a metabolic gradient within the lens since, in general, the concentration of metabolites in the central region, the nucleus, is significantly less than in the more metabolically active outer cortex. Lens fiber cells develop extensive intercellular communication pathways through gap junctions and lose all intracellular membranes, and hence, it would seem reasonable to expect the lens as a whole to behave like a syncytium. Since this is not the case, one means of achieving compartmentation of lens metabolic activity could be by specific or nonspecific metabolite binding to enzymes or lens structural proteins. This is a

† This research was supported by National Institutes of Health Grants EY 04033 and EY 05787.

* Author to whom correspondence should be addressed.

‡ University of California.

§ Present address: CIBA Vision, 5000 McGinnis Ferry Rd., Alpharetta, GA 30201.

‖ University of Medicine and Dentistry—New Jersey Medical School.

[1] Abbreviations: NMR, nuclear magnetic resonance; D_R, rotational diffusion coefficient; DD, dipole–dipole; CSA, chemical shift anisotropy; FIR, fast inversion recovery; FID, free induction decay; ppm, parts per million; T_1, longitudinal (spin–lattice) relaxation time; T_2, transverse relaxation time; NOE, nuclear Overhauser enhancement; rf, radiofrequency; HSVD, Hankel singular value decomposition; PME, phosphomonoester; P_i, inorganic phosphate; PCr, phosphocreatine; GPC, L-α-glycerophosphocholine; NTP, nucleotide triphosphate; NDP, nucleotide diphosphate; ATP, adenosine triphosphate; ADP, adenosine diphosphate; DN, dinucleotide; UDPG, uridinediphosphoglucose; G-3-P, L-α-glycerol phosphate; 2,3-BPG, 2,3-bisphosphoglycerate; BSA, bovine serum albumin.

0006-2960/90/0429-7547$02.50/0

reasonable hypothesis since the lens contains an inordinately high concentration of protein (300–400 g L^{-1}) which is predominantly composed of the α-, β-, and γ-crystallins [for reviews see Zigler and Goosey (1981) and Harding and Crabbe (1984)]. There is evidence for the binding of G-3-P, a major lens metabolite, to γ-crystallin under pH and ionic conditions similar to those encountered physiologically (Groth-Vaselli et al., 1988). This is similar to the preferential binding of 2,3-BPG to the deoxy form of hemoglobin in erythroid cells (Benesch & Benesch, 1967). It is well established that fluctuations in the free intracellular concentration of 2,3-BPG exert considerable effect on red cell metabolic regulation (Hathaway & Trough, 1984).

The purpose of this study was to investigate phosphorus metabolite rotational diffusion in bovine (calf) lens homogenates, and to use the results to estimate the occurrence and extent of metabolite lens protein interactions. A commonly held tenet of in vivo NMR spectroscopy is that only free or unbound tissue phosphorus metabolites are detected. However, it is likely that a fraction of the phosphorus metabolites present in lens tissue are protein bound in a correlation time range which still permits detection by high-resolution NMR spectroscopic techniques. Rotational diffusion measurements, which appear not to have been performed for tissue metabolites, complement recently reported pulse gradient spin-echo translational diffusion measurements of phosphorus metabolites in intact tissue (Yoshizaki et al., 1982; Moonen et al., 1990). The combination of rotational and translation diffusion data provides important information about intracellular molecular motion, permitting insight into the nature of cytoplasmic dynamics as it relates to organization and structure and, in the case of the lens, transparency. The NMR spectroscopic technique, off-resonance rotating frame spin–lattice relaxation (James, 1984; Schleich et al., 1989a), was used to determine the rotational diffusion behavior of phosphorus metabolites in calf lens tissue homogenates. This NMR technique is suitable for noninvasive studies of molecular rotational motion in the range of 1 to hundreds of nanoseconds and has proved useful for the study of the lens protein rotational diffusion in calf lens cortical and nuclear homogenates (Morgan et al., 1989). That study established the presence of both mobile and solidlike protein phases in the lens nucleus, whereas for the cortex, within the detection limits of NMR, the protein phase was found to be mobile.

In the present study the occurrence and extent of phosphorus metabolite–lens protein interactions in calf lens cortex and nuclear homogenates, above and below the cold cataract phase transition temperature (Clark & Benedek, 1980), was investigated by the determination of the rotational correlation time ($\tau_0 = 1/6D_R$) for key lenticular phosphorus metabolites. The spectral intensity ratio dispersion curves, derived from the ^{31}P NMR metabolite resonances as a function of offset frequency (dispersion), were analyzed by using a two-site fast-exchange model to estimate the extent of protein-bound (i.e., slower) rotationally diffusing metabolites.

Theory

The theoretical formalism of the off-resonance rotating frame spin–lattice relaxation experiment has been presented by James (1984) and Schleich et al. (1989a).

In this experiment the application of continuous wave, off-resonance, low rf power irradiation is used to produce a *field of amplitude* B_2 that is off-resonance from the resonance of interest by an offset frequency Δ ($=2\pi\nu_{off}$). The effective field, $\mathbf{B}_e$, established in the rotating frame, is inclined to the static magnetic field, $\mathbf{B}_0$, at an angle Θ defined by $\tan\Theta = \gamma B_2/\Delta$. The nuclear spins precess about $\mathbf{B}_e$ with an angular velocity of magnitude ω_e ($=\Delta/\cos\Theta$).

The spectral intensity ratio [$R = (\cos^2\Theta)T_{1\rho}^{off}/T_1$] is experimentally determined as a function of the offset frequency (dispersion) from the observed signal intensity ratio (M_{eff}/M_0), where M_{eff} and M_0 are the equilibrium magnetizations established in the presence and absence of an applied off-resonance B_2 field, respectively. M_0 is the steady-state magnetization attained along $\mathbf{B}_0$, and M_{eff} is the corresponding magnetization along $\mathbf{B}_e$. Thus, M_{eff} ($\leq M_0$) approaches M_0 in the limit of very far off-resonance (large offset frequency).

^{31}P NMR relaxation studies of 2,3-BPG, a representative tissue metabolite, conducted in aqueous solution and in the intact erythrocyte indicate that dipole–dipole and chemical shift anisotropy relaxation mechanisms are dominant at the high B_0 field employed in this study (Christensen & Jacobsen, 1988) and were therefore assumed in the data analysis. Isotropic metabolite tumbling was also assumed. A review of ^{31}P nuclear spin relaxation mechanisms has been published by McCain (1987); the use of NMR in the investigation of protein–phosphorus interactions has been discussed by Brauer and Sykes (1987).

The total dipole–dipole relaxation rate is the sum of the intramolecular rotational and intermolecular translational contributions. For intramolecular dipole–dipole interactions between proton and phosphorus nuclei, and spin–lattice relaxation expressions are

$$\left(\frac{1}{T_1}\right)^{HP}_{DD,rot} = \sum_1^H K[J_0(\omega_H - \omega_P) + 3J_1(\omega_P) + 6J_2(\omega_H + \omega_P)] \quad (1)$$

$$\left(\frac{1}{T_{1\rho}^{off}}\right)^{HP}_{DD,rot} = \left(\frac{1}{T_1}\right)^{HP}_{DD,rot} + (\sin^2\Theta)\sum_1^H K\left\{2J_0(\omega_e) + \frac{3}{2}[J_1(\omega_H + \omega_e)] + \frac{3}{2}[J_1(\omega_H - \omega_e)]\right\} \quad (2)$$

with $K = \hbar^2\gamma_H^2\gamma_P^2/20r_{HP}^6$, where $\hbar$ is Planck's constant divided by 2π, γ_H and γ_P are the gyromagnetic ratios for ^1H and ^{31}P, r_{HP} is the internuclear distance between the phosphorus and the particular proton responsible for dipolar relaxation, and H is the number of protons. $J(\omega_i)$ is the spectral density function; ω_H and ω_P are the respective proton and phosphorus Larmor precessional frequencies.

The expressions for intramolecular dipole–dipole spin–lattice relaxation between phosphorus nuclei are

$$\left(\frac{1}{T_1}\right)^{PP}_{DD,rot} = \sum_1^P K_P[J_1(\omega_P) + 4J_2(2\omega_P)] \quad (3)$$

$$\left(\frac{1}{T_{1\rho}^{off}}\right)^{PP}_{DD,rot} = \left(\frac{1}{T_1}\right)^{PP}_{DD,rot} + (\sin^2\Theta)\sum_1^P K_P\left\{\frac{3}{2}J_0(\omega_e)\right\} \quad (4)$$

where $K_P = 3\hbar^2\gamma_P^4/20r_{PP}^6$, r_{PP} is the internuclear distance between the phosphorus nuclei, and P is the number of phosphorus atoms.

In biological samples nuclear spins occur in different microenvironments, thus leading to a distribution of relaxation times. In this study we have assumed for simplicity a single (average) rotational correlation time to characterize reorientational motion.

The spectral density function for dipolar relaxation is defined by

$$J_n(\omega) = \langle A(0)A(p)\rangle \frac{2\tau_0}{(1 + \omega^2\tau_0^2)} \quad (5)$$

where $\langle A(0)A(p)\rangle$ is the plateau amplitude at time p, the time when internal molecular motion averaging is finished, but before significant rotational motion has commenced (i.e., $p \ll \tau_0$), and τ_0 is the correlation time for isotropic reorientational motion of a rigid spherical particle (Levy et al., 1981; McCain & Markley, 1986). Since a spectral intensity ratio, and hence, a ratio of spectral densities, is measured in our implementation of the off-resonance rotating frame spin–lattice relaxation experiment (vide ante), the constant plateau amplitude factor of each spectral density contribution cancel as is the case for the NOE experiment (McCain & Markley, 1986).

The off-resonance rotating frame spin–lattice relaxation experiments reported in this study were performed in H_2O. In this case it is necessary to consider intermolecular contributions to the total dipole–dipole relaxation rate of a phosphorus metabolite arising from solvent (water) translational motion. The theoretical translational contribution to the dipole–dipole relaxation rate was evaluated by using the simple model of Abragam (1961) which assumes Brownian diffusion of a particle through a homogeneous viscous fluid medium. For the heteronuclear case, where one of the spins is very dilute relative to the other, we obtain in the extreme narrowing limit ($\omega^2\tau^2 \ll 1$)

$$\left(\frac{1}{T_1}\right)^{HP}_{DD,trans} = \hbar^2\gamma_H^2\gamma_P^2 2\pi(2N/15dD) \quad (6)$$

where N is the solvent proton number density in the solution, d is the P–H distance of closest approach, and D is the average of the water and phosphorus metabolite diffusion coefficients. For translation τ is defined to be $d^2/2D$. A similar equation, differing by a factor of 2π, was derived by McCain and Markley (1980).

Similarly for the off-resonance rotating frame spin–lattice relaxation rate the following expression was derived:

$$\left(\frac{1}{T_{1\rho}^{off}}\right)^{HP}_{DD,trans} = \hbar^2\gamma_H^2\gamma_P^2\pi(2 + \sin^2\Theta)(2N/15dD) \quad (7)$$

Since the angle Θ in the off-resonance experiment is small, $(1/T_{1\rho}^{off})^{HP}_{DD,trans} \approx (1/T_1)^{HP}_{DD,trans}$, as would be expected in the extreme narrowing limit.

In addition to nuclear dipole–dipole relaxation, the anisotropic chemical shift of the phosphoryl group significantly contributes to the phosphorus relaxation at the high magnetic field used in this study and was thus taken into account.

$$\left(\frac{1}{T_1}\right)_{CSA} = \frac{3}{20}(\gamma_P^2 B_0^2 \delta_z^2)\sum_{j=0}^{2} J_j(\omega) \quad (8)$$

$$\left(\frac{1}{T_{1\rho}^{off}}\right)_{CSA} = \left(\frac{1}{T_1}\right)_{CSA} + \frac{1}{10}(\gamma_P^2 B_0^2 \delta_z^2)(\sin^2\Theta)\sum_{j=0}^{2} J_j(\omega_e) \quad (9)$$

where δ_z is the anisotropy factor. The spectral density function for CSA relaxation is given by

$$J_j(\omega) = \langle A(0)A(p)\rangle \frac{2c_j\tau_j}{(1 + \omega^2\tau_j^2)} \quad (10)$$

where $\tau_j = \tau_0$ for $j = 0, 1, 2$ (isotropic motion), with $c_0 = 1$, $c_1 = 0$, and $c_2 = \eta^2/3$, where η is the asymmetry parameter.

The total relaxation rate was obtained by summing the individual relaxation rates contributed by the different assumed mechanisms.

$$\frac{1}{T_1} = \left(\frac{1}{T_1}\right)^{HP}_{DD,rot} + \left(\frac{1}{T_1}\right)^{PP}_{DD,rot} + \left(\frac{1}{T_1}\right)^{HP}_{DD,trans} + \left(\frac{1}{T_1}\right)_{CSA} \quad (11a)$$

$$\frac{1}{T_{1\rho}^{off}} = \left(\frac{1}{T_{1\rho}^{off}}\right)^{HP}_{DD,rot} + \left(\frac{1}{T_{1\rho}^{off}}\right)^{PP}_{DD,rot} + \left(\frac{1}{T_{1\rho}^{off}}\right)^{HP}_{DD,trans} + \left(\frac{1}{T_{1\rho}^{off}}\right)_{CSA} \quad (11b)$$

Dipolar relaxation contributions from phosphorus metabolite bound Mg^{2+} were ignored in the data analysis as were paramagnetic ion contributions (vide infra).

The magnetization behavior of the off-resonance experiment including the effects of saturation transfer (assuming exchange between two sites, A and B, and the absence of cross-relaxation) has been analyzed by Schleich et al. (1989b). In this situation the spectral intensity ratio (R) is given by $(\cos^2\Theta)(T_{1\rho}^{off}/T_1)(1 - k_A\tau_{1A})$, where k_A is the rate constant for exchange from A to B, $1/\tau_{1A} = 1/T_{1\rho}^{off} + 1/\tau_A$, and $1/\tau_A = k_A$. Thus, a plot of R vs ω_e will plateau at R values that are less than unity when saturation transfer effects are operant.

Experimental Procedures

NMR Measurements. ^{31}P NMR spectra were obtained at 121.48 MHz by using a General Electric GN-300 spectrometer equipped with a Oxford Instruments 7.05-T, wide-bore (89-mm) magnet. A GE 20-mm broad-band probe and 20 mm (o.d.) NMR tubes (nonspinning) were used for the off-resonance rotating frame spin–lattice relaxation experiments. The low-power off-resonance B_2 field, provided by the X-nucleus broad-band decoupler, was continuously applied for 20 s (at least 4 T_1) between acquisitions. To eliminate residual power interference effects from the broad-band decoupler when gated off, four pairs of crossed diodes (1N914) and a low band filter were used in line between the decoupler and the preamplifier (probe interface module). The B_2 field strength, typically 0.2–0.4 G, was calibrated with an aqueous solution of Na_2HPO_4 (100 mM) and NaCl (150 mM). The B_2 offset frequencies (ν_{off}) ranged from 1 to 35 kHz. Reference spectra were obtained with a resonance offset of 300 kHz. Typical parameters were as follows: 90° pulse width, 48 μs; 4096 data points per free induction decay (FID); sweep width ±3000 Hz (quadrature phase detection). Phase cycling was employed to minimize baseline spectral artifacts. Zero filling and 20-Hz line broadening were employed prior to Fourier transformation. To minimize the impact of slow metabolite level changes with time, the total number of transients (100, cortical; 200, nuclear) at the particular offset frequency and the corresponding reference frequency were collected by alternating between the two in blocks of 20 accumulations. A randomly selected order of frequency offsets was used. Sample temperature was regulated to within ±0.5 °C of the desired value.

Spin–lattice relaxation times of phosphorus metabolites present in cortical and nuclear homogenates were measured by fast inversion recovery (Schleich et al., 1984); 32 different delay times (τ) were used. The pulse delay time was 4.8 s.

The spectral acquisition parameters previously noted were employed, with the following exceptions: for each of the 32 spectra, a total of 240 FID's were collected in blocks of 20 accumulations, with 2048 data points per FID. A sample temperature of 5 °C was used as a means of stabilizing phosphorus metabolite levels in the lens homogenates.

$^{31}P\{^1H\}$ NOE values for phosphorus metabolites were determined by gated broad-band proton decoupling. The proton irradiation time prior to ^{31}P spectral acquisition was 60 s, which represented a minimum of 9–10 times the longest ^{31}P T_1 value. Proton rf power levels were adjusted to maximize the NOE. Spectral acquisition parameters as noted above were employed with the following exceptions: a total of 580 FID's were collected at 5 °C with 4096 data points per FID. The proton-irradiated and control spectral acquisitions were interleaved.

^{13}C off-resonance rotating frame spin–lattice relaxation experiments for the determination of lens protein homogenate rotational diffusion characteristics were performed at 7.05 T as previously described (Morgan et al., 1989; Schleich et al., 1989a).

Lens Homogenate Preparation. Calf eyes (1–3 day old calves) were obtained from a local slaughterhouse and kept on ice until the lenses were dissected out, and the homogenates were prepared, as previously described (Morgan et al., 1989).

Data Analysis. ^{31}P resonance assignments were made as previously described (Schleich et al., 1985). Chemical shift values were expressed relative to internal GPC (0.49 ppm). The ^{31}P NMR spectra were analyzed by line-shape deconvolution using the GE GEMCAP software routine to provide the relevant ^{31}P resonance intensities. The ^{13}C NMR spectra were analyzed by integration of the protein carbonyl resonance envelope. The signal intensity ratios were calculated from the observed signal intensities (see Theory).

Values of effective correlation times ($\tau_{0,eff}$) were obtained by nonlinear least-squares regression of R vs ω_e data using the NONLINWOOD routine (Daniel & Wood, 1980). Intramolecular DD and CSA relaxation and solvent translational intermolecular DD relaxation contributions, as described above, were incorporated in the nonlinear routine. Only intermolecular DD relaxation and CSA relaxation contributions were assumed in the analysis of P_i. The analyses assumed random isotropic rotational motion and lead to a mean rotational correlation time, $\tau_{0,eff}$ (Schleich et al., 1989a). The fraction of free and bound phosphorus metabolite was obtained by nonlinear regression analysis of R vs. ω_e curves, assuming eq 12, by constraining $\tau_{0,free}$ and $\tau_{0,bound}$ to the values obtained as described below. The expressions in eqs 12a and 12b describe two-site fast-exchange averaging of the spin–lattice relaxation times between the free and macromolecular bound environments of the phosphorus metabolites. The fractional amounts of a particular metabolite are represented by Θ_{free} and Θ_{bound} and sum to unity.

$$\frac{1}{T_1} = \frac{\Theta_{free}}{T_{1,free}} + \frac{\Theta_{bound}}{T_{1,bound}} \quad (12a)$$

$$\frac{1}{T_{1\rho}^{off}} = \frac{\Theta_{free}}{T_{1\rho,free}^{off}} + \frac{\Theta_{bound}}{T_{1\rho,bound}^{off}} \quad (12b)$$

Through-space internuclear distances, used in calculating the DD interaction contributions, were obtained from energy-minimized chemical structures generated with Alchemy computer graphics software (Tripos Associates). Proton DD relaxation contributions to calculated T_1 and $T_{1\rho}^{off}$ values of a particular metabolite included all nonexchangeable proton–phosphorus distances, whereas for ATP phosphorus–phosphorus distances were also included.

Principal values of the ^{31}P chemical shift tensors were used to determine values for the asymmetry parameter, η, and the anisotropy factor, δ_z, following established procedures (Gerstein & Dybowski, 1985). The CSA tensor of the compounds in parentheses were used as representative models for the phosphorus metabolites studied: PME [L-α-glycerol phosphate (Kohler & Klein, 1976)]; GPC [L-α-glycerophosphocholine; (Kohler & Klein, 1976)]; P_i [ab initio quantum mechanical calculations (Prado et al., 1979); KH_2PO_4 (Terao & Hashi, 1974)]; ATP [sodium pyrophosphate (Shriver & Sykes, 1981)].

Isotropic rotational correlation times for the free (unbound) metabolites, $\tau_{0,free}$, were calculated by using the Stokes–Einstein equation ($\tau_{0,free} = 4\pi a^3\eta/3kT$), where η is the viscosity, a is the molecular radius, k is Boltzmann's constant, and T is the absolute temperature. Estimated values of the lens cytoplasmic viscosity were 1.7 (cortical) and 2.4 (nuclear) times that of pure water at the desired temperature (Morgan et al., 1989). For bound metabolite, $\tau_{0,bound}$ was set equal to the lens protein $\tau_{0,eff}$ value obtained by ^{13}C off-resonance rotating frame spin–lattice relaxation under the desired condition. Values of the self-diffusion coefficient of water in cortical and nuclear homogenates were taken from Haner et al. (1989). Estimates of molecular radii were made with Alchemy software.

Inversion–recovery magnetization data were first analyzed by application of an HSVD algorithm (Barkhuijsen et al., 1987) to establish the number of time-dependent components from a plot of singular values as a function of array index. Spin–lattice relaxation times were subsequently determined by nonlinear least-squares regression employing the function (Crouch et al., 1982; Levy & Peat, 1975):

$$M(\tau) = M_\infty\{1 - [1 + W[1 - \exp(-PD/T_1)]] \exp(-\tau/T_1)\}$$

where W is a term which compensates for inhomogeneous B_1 fields and PD is the pulse delay time between successive 180°–τ–90° pulse sequences. Theoretically, $W = 1$; typical values were 0.86–0.94.

Results

Simulations. The utility of the off-resonance rotating frame spin–lattice relaxation technique for the investigation of phosphorus metabolite rotational diffusion is illustrated in Figure 1A. This figure compares the computer-simulated signal intensity ratio dispersion curves, R vs ω_e, for different values of the rotational correlation time. The family of curves, depicted by the solid lines, was generated for an isotropically tumbling phosphorus metabolite, assuming both intramolecular DD and CSA relaxation mechanism contributions, whereas the dotted lines include in addition a relaxation contribution from solvent translational motion. Both simulations employed parameters characteristic of a phosphomonoester (stated in the figure legend). With increasing correlation time the attainment of the maximum value of the spectral intensity ratio (at constant off-resonance irradiation field strength) requires larger values of ν_{off}. As shown in Figure 1A, a wide range of rotational correlation times from less than a nanosecond to at least 100 ns may be investigated. Changing the off-resonance irradiation field strength alters the window of rotational motion sensitivity slightly. The theoretical contribution of solvent translational motion to the intramolecular DD spin–lattice relaxation rate was assessed for PME by using eq 6. The value 2.09 Å was used for d (McCain & Markley, 1980), and N was the pure solvent value (6.75×10^{22} protons/cm^3). The average translational diffusion coefficient was estimated by using the Stokes–Einstein equation to calculate the PME translational diffusion coefficient from τ_0, assuming the vis-

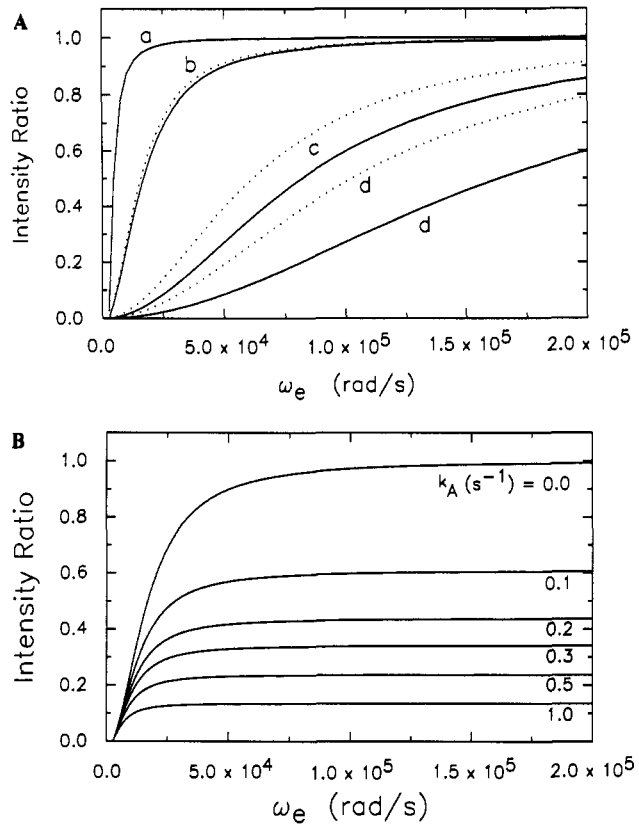

FIGURE 1: (A) Simulated intensity ratio dispersion curves as a function of isotropic rotational correlation time [(a) 1.0 ns; (b) 10.0 ns; (c) 50.0 ns; (d) 100.0 ns] for G-3-P. A B_0 field of 7.05 T, an off-resonance B_2 field of 0.25 G, DD relaxation by two protons located 2.6 Å from the ^{31}P, and CSA relaxation (−58.33 ppm for δ_z and −0.67 for η) were assumed (solid lines). The dotted lines indicate the effect of an additional intermolecular DD relaxation contribution from solvent (water) translational motion at 20 °C to the G-3-P-simulated intensity ratio dispersion curves (see text for details). (B) ^{31}P-simulated intensity ratio dispersion curves for G-3-P as a function of the forward exchange rate (k_A) assuming two-site metabolite exchange between a "mobile" (site A) and an "immobile" (site B) saturated species. A τ_0 value of 10 ns was assumed. Other NMR parameters are listed in (A).

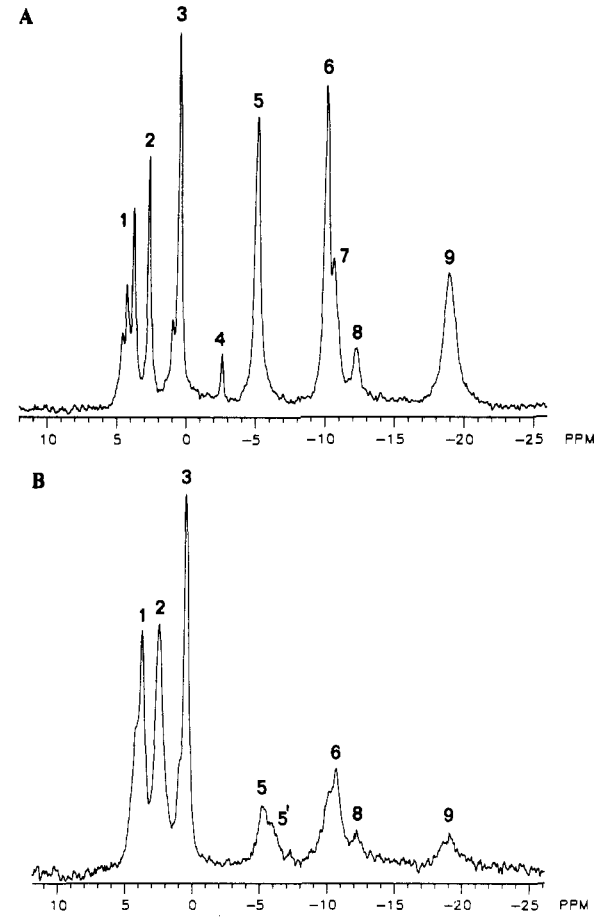

FIGURE 2: ^{31}P NMR spectra of calf (A) cortical homogenate, 100 transients, and (B) nuclear homogenate, 200 transients at 10 °C. Resonance assignments are as follows: (1) PME; (2) P_i; (3) GPC; (4) PCr; (5) γ-NTP; (5′) β-NDP; (6) α-NTP, α-NDP; (7) DN; (8) UDPG; (9) β-NTP. In lens, the predominant contributions to the PME and NTP (NDP) resonances are from L-α-glycerol phosphate and ATP (ADP), respectively (Harding & Crabbe, 1984). A 10-Hz line-broadening factor was used prior to Fourier transformation. Other spectral acquisition parameters are noted under Experimental Procedures.

cosity value and self-diffusion coefficient of pure water at 20 °C. For a particle of τ_0 = 10 ns we calculated a $(1/T_1)^{HP}_{DD,trans}$ value of ca. 2.4×10^{-2} s^{-1} for PME in water. This value is equal to 0.6 times the intramolecular relaxation rate contribution and is ca. 0.2 times the CSA contribution. As shown by the family of dotted lines in Figure 1A, the effect of solvent translational motion is negligible at short τ_0 values (≤10 ns) but assumes increasing significance as τ_0 increases. The effect of solvent translation motion is to shift the R vs ω_e curves to a smaller τ_0 value. It should be noted that even for a large isotropically tumbling particle in water at 20 °C, with a rotational correlation time of 100 ns (the average translational diffusion coefficient equals 1.05×10^{-5} cm^2/s), $\omega^2\tau^2$ equals 1.1×10^{-3}, thereby fulfilling the assumption of "extreme narrowing" used in the derivation of eq 6. Thus, a solvent translation DD relaxation contribution is also significant for protein-bound ligand.

The off-resonance rotating frame spin–lattice relaxation theory was modified to include the effects of saturation transfer kinetics (adopting two-site exchange) between a mobile (NMR-"visible") and a relatively immobile (NMR-"invisible") pool of metabolites. Since the immobile pool is easily saturated (because of a long T_1), the analysis of R vs ω_e data with the modified theory is appropriate in those instances where the limiting value of unity for $R_{\omega=\infty}$ is not attained (Schleich et al., 1989b). Figure 1B shows a family of curves generated at a constant τ_0 value, but with varying values of k_A, the rate constant for exchange from the mobile pool (site A) to the immobile pool (site B). With increasing exchange, i.e., increasing values of k_A, the limiting value of $R_{\omega=\infty}$ decreases from unity.

Cortical Homogenate. The ^{31}P NMR spectrum of calf lens cortical homogenate at 10 °C is shown in Figure 2A and represents the NMR-"visible" phosphorus metabolites. Phosphorus metabolite line widths ranging from ca. 18–22 Hz (P_i, GPC, and PME) to 44–50 Hz (α- and γ-ATP resonances) were obtained. The β-ATP resonance was observed to be considerably broader (110 Hz). The spectral intensity ratio dispersion curves, R vs ω_e, for the phosphoryl resonances of ATP, GPC, and P_i in calf lens cortical homogenate at 10 °C are shown in Figures 3 and 4. The metabolites studies were GPC, PME, P_i, and ATP. In lens, the predominant contribution to the PME and NTP (NDP) resonances are from L-α-glycerol phosphate and ATP (ADP), respectively (Harding & Crabbe, 1984). The fitted curves (represented by the solid lines), using an isotropically tumbling metabolite model in the nonlinear regression analysis, provided values for *effective* rotational correlation times ($\tau_{0,eff}$) of the individual metabolites. Values of $\tau_{0,eff}$ are listed in Tables I and II at the two temperatures investigated in this study, 10 and 18 °C. The different phosphorus metabolites present in cortical lens homogenate varied in $\tau_{0,eff}$ values, ranging from ca. 2 (GPC) to 12 ns (ATP). These $\tau_{0,eff}$ values, in each case, were substantially

Table I: Correlation Times and Limiting Spectral Intensity Ratios for Calf Lens Homogenate Phosphorus Metabolites at 10 °C

	cortical			nuclear		
metabolite	$\tau_{0,eff}$[a]	τ_{free}[b]	$R_{\omega=\infty}$	$\tau_{0,eff}$[a]	τ_{free}[b]	$R_{\omega=\infty}$
GPC	1.6 ± 0.2	0.09	0.97 ± 0.01	2.9 ± 0.1	0.15	1.00 ± 0.01
PME	4.4 ± 0.5	0.15	1.02 ± 0.03	17.2 ± 1.8	0.22	0.99 ± 0.03
P_i	10.6 ± 0.5	0.01	0.96 ± 0.02	40.7 ± 2.3	0.01	1.07 ± 0.03
α-ATP	12.2 ± 1.0	0.98	0.94 ± 0.03			
β-ATP	11.3 ± 0.8	0.98	1.06 ± 0.03			
γ-ATP	10.3 ± 0.9	0.98	0.96 ± 0.03			

[a] Obtained by nonlinear regression of R vs ω_e dispersion curves. See text for details. [b] Calculated η_0(cytoplasm) = $\chi\eta_0(H_2O)$: χ = 1.66 (cortical); χ = 2.43 (nuclear).

Table II: Correlation Times and Limiting Spectral Intensity Ratios for Calf Lens Homogenate Phosphorus Metabolites at 18 °C

	cortical			nuclear		
metabolite	$\tau_{0,eff}$[a]	τ_{free}[b]	$R_{\omega=\infty}$	$\tau_{0,eff}$[a]	τ_{free}[b]	$R_{\omega=\infty}$
GPC	1.3 ± 0.2	0.08	0.97 ± 0.01	3.7 ± 0.2	0.12	1.01 ± 0.01
PME[c]	6.6 ± 0.7	0.12	0.90 ± 0.04	25.5 ± 1.4	0.17	0.93 ± 0.02
P_i	8.9 ± 0.2	0.01	0.99 ± 0.01	38.7 ± 2.4	0.01	1.07 ± 0.03
α-ATP[c]	6.6 ± 1.0	0.77	0.87 ± 0.04			
β-ATP						
γ-ATP	8.9 ± 1.1	0.77	1.01 ± 0.04			

[a] Obtained by nonlinear regression of R vs. ω_e dispersion curves. See text for details. [b] Calculated η_0(cytoplasm) = $\chi\eta_0(H_2O)$: χ = 1.66 (cortical); χ = 2.43 (nuclear). [c] Obtained by nonlinear regression of R vs. ω_e dispersion curves using off-resonance rotating frame spin-lattice relaxation formalism modified to include chemical exchange effects (Schleich et al., 1989b). See text for details. Exchange rate constants (k_A) are noted in Results.

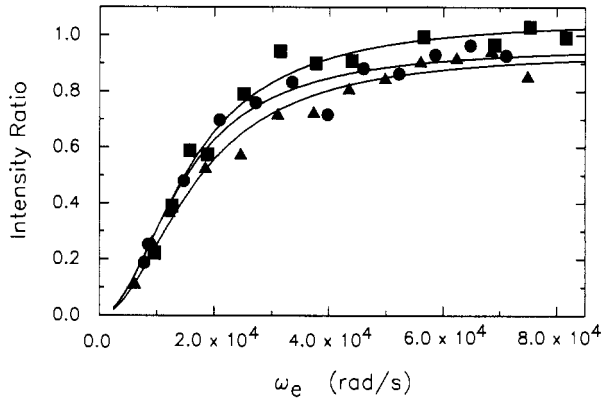

FIGURE 3: ^{31}P spectral intensity ratio dispersion curves for the α- (▲), β- (■), and γ- (●) ATP resonances present in calf lens cortical homogenate at 10 °C. The solid lines represent the best fit obtained by nonlinear regression assuming an isotropic reorientation model. Intra- and intermolecular DD and CSA relaxation mechansim contributions were assumed. See text for details. Spectral acquisition parameters are noted under Experimental Procedures.

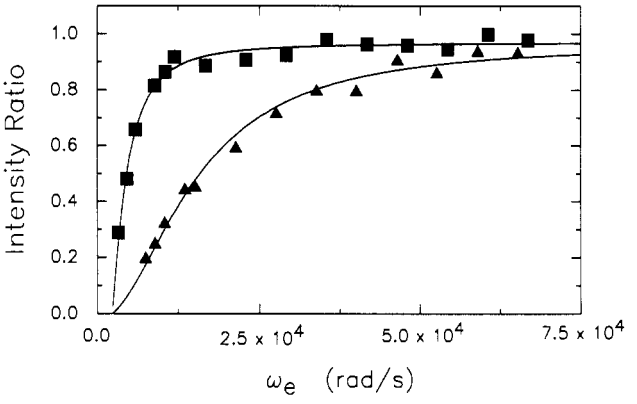

FIGURE 4: ^{31}P spectral intensity ratio dispersion curves for the GPC (■) and P_i (▲) resonances present in calf lens cortical homogenate at 10 °C. The solid lines represent the best fit obtained by nonlinear regression assuming an isotropic reorientation model. Intra- and intermolecular DD and CSA relaxation mechanism contributions were assumed. See text for details. Spectral acquisition parameters are noted under Experimental Procedures.

larger than what would be expected from the rotational diffusion of a free, or unbound, metabolite in an environment of enhanced viscosity characteristic of lens cytoplasm. With the exception of PME and the α-ATP resonance at 18 °C, the limiting value of the fitted spectral intensity ratio ($R_{\omega=\infty}$) was at least 0.94. For these metabolites the modified formalism of the off-resonance rotating frame spin–lattice relaxation theory, which incorporates exchange with a saturated NMR-"invisible" metabolite pool, was used to fit the data (Schleich et al., 1989b). Values of k_A of (2.9 ± 1.4) × 10^{-2} s^{-1} (PME) and (5.5 ± 2.5) × 10^{-2} s^{-1} (α-ATP + α-ADP) at 18 °C were obtained ($\tau_{0,eff}$ values are listed in Table II) and represent the exchange rate of the metabolite from the "visible" into the "invisible" pool. A change in temperature from 10 to 18 °C resulted in no significant change in $\tau_{0,eff}$ for GPC, whereas for PME the change was *opposite* in direction to that expected for an increase in temperature, and for P_i and ATP the change in the expected direction was obtained. Theoretically, for rotational diffusion, if the viscosity–temperature dependence of water is assumed, and the change in temperature is taken into account, an increase by a factor of 1.28 is expected for a temperature change from 18 to 10 °C.

Measurements of average protein reorientational motion by ^{13}C off-resonance rotating frame spin–lattice relaxation methodology gave $\tau_{0,eff}$ values of 96.3 ± 5.4 and 126.3 ± 8.0 ns at 18 and 10 °C, respectively, for the cortical homogenate preparations used in this study.

The fraction of free metabolites is tabulated in Tables III and IV for cortical homogenate, at both 10 and 18 °C (below and above the cold cataract phase transition temperature). Assuming binding to the entire lens protein population, i.e., employing the experimentally determined value of $\tau_{0,eff}$ for the lens proteins in the homogenate, the fraction of free GPC, PME, and P_i was observed to be greater than 0.9, whereas for ATP the average value was lower at both temperatures. However, at 10 °C the fraction of free ATP is less than at 18 °C. The assumption of a "structure-making" model (McCain & Markley, 1980) for DD relaxation in P_i in place of solvent translation resulted in no change in Θ_{free}.

Nuclear Homogenate. The ^{31}P NMR spectrum of calf lens

Table III: Fraction of Free Phosphorus Metabolite in Calf Lens Homogenate at 10 °C

meta-bolite	Θ_{free}[a] (cortical)	Θ_{free}[a] (nuclear)	meta-bolite	Θ_{free}[a] (cortical)	Θ_{free}[a] (nuclear)
GPC	0.98	0.98	α-ATP	0.72	
PME	0.97	0.80	β-ATP	0.74	
P_i	0.99	0.84	γ-ATP	0.78	

[a] Estimated uncertainty is ±10%.

Table IV: Fraction of Free Phosphorus Metabolite in Calf Lens Homogenate at 18 °C

meta-bolite	Θ_{free}[a] (cortical)	Θ_{free}[a] (nuclear)	meta-bolite	Θ_{free}[a] (cortical)	Θ_{free}[a] (nuclear)
GPC	0.98	0.96	α-ATP	0.90	
PME	0.92	0.63	β-ATP		
P_i	0.99	0.87	γ-ATP	0.79	

[a] Estimated uncertainty is ±10%.

nuclear homogenate at 10 °C is shown in Figure 2B and represents the NMR-"visible" phosphorus metabolites. Phosphorus line widths of 23–24 Hz (GPC, PME) and 55 Hz (P_i) were obtained for phosphorus metabolites present in calf lens nuclear homogenates at 10 °C. Phosphoryl resonance spectral intensity ratio dispersion curves for GPC and PME in calf nuclear lens tissue, R vs ω_e, obtained at 18 °C are shown in Figure 5. In this case, only the PME, P_i, and GPC metabolites could be studied, since the α-, β-, and γ-ATP resonances were significantly lower in signal intensity. This observation is in accord with the finding of Greiner et al. (1985) that the amount of ATP in the lens nucleus is ca. one-third that found in the cortex, the result of substantially diminished metabolism in the nucleus. For calf nuclear lens tissue, a cold cataract phase transition occurs at ca. 16 °C (Clark & Benedek, 1980) resulting in intense light scattering. Thus, the two temperatures employed in this study, 10 and 18 °C, represent values below and above the cold cataract phase transition temperature. Cortical material does not sustain a cold cataract phase transition. Values of $\tau_{0,eff}$ for the metabolites found in calf lens nuclear homogenate at 10 and 18 °C are listed in Tables I and II. Metabolite $\tau_{0,eff}$ values ranged from ca. 3 ns (GPC) to 41 ns (P_i). The $\tau_{0,eff}$ values for GPC and PME were larger at 18 °C than at 10 °C, a result *opposite* to what would be expected for a simple change in temperature (vide supra), wheras $\tau_{0,eff}$ for P_i was somewhat larger at 10 °C than at 18 °C. The limiting value of the fitted spectral intensity ratio dispersion curves in each case attained a value of at least 0.99, with the exception of PME at 18 °C. A value of k_A equal to $(7.6 \pm 2.6) \times 10^{-3}$ s^{-1} was obtained for the exchange rate.

Nuclear homogenate lens proteins were characterized by $\tau_{0,eff}$ values of 113.5 ± 10.8 and 128.4 ± 8.9 ns at 18 and 10 °C, respectively, as assessed by the ^{13}C off-resonance rotating frame spin–lattice relaxation experiment.

Comparison of $\tau_{0,eff}$ values obtained for the metabolites GPC, PME, and P_i present in the nuclear vs the cortical lens regions showed an increase of ca. 3- to 4-fold at 18 °C, and ca. 2- to 4-fold at 10 °C.

For nuclear homogenate, the fractions of free GPC and P_i (see Tables III and IV) were essentially temperature independent, with the exception of PME, chiefly represented by G-3-P, which was less bound at a temperature below the cold cataract phase transition temperature than above. Such temperature-dependent binding is consistent with the observed binding behavior of G-3-P to γ-crystallin (Groth-Vaselli et al., 1988). Substitution of a "structure-making" model for solvent translational motion mediated DD relaxation produced an 8% decrease in the fraction of free P_i.

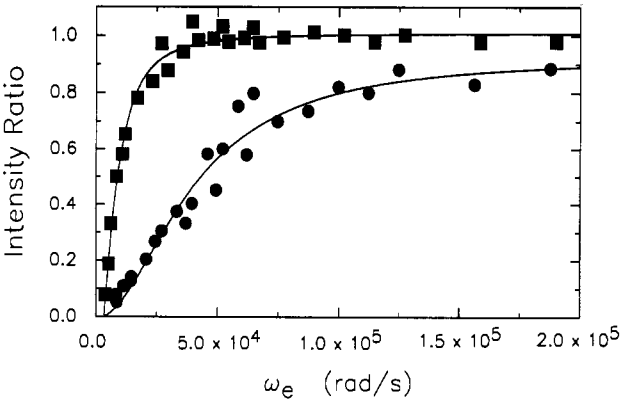

FIGURE 5: ^{31}P spectral intensity ratio dispersion curves for the GPC (■) and PME (●) resonances present in calf lens nuclear homogenate at 18 °C. The solid lines represent the best fit obtained by nonlinear regression assuming an isotropic reorientation model. Intra- and intermolecular DD and CSA relaxation mechanism contributions were assumed. See text for details. Spectral acquisition parameters are noted under Experimental Procedures.

Spin–Lattice Relaxation Measurements. Phosphorus metabolite T_1 values in the range of seconds for metabolites present in both cortical and nuclear homogenates were obtained at 5 °C; numerical values and the relevant statistical parameters are listed in Table V. In each case the FIR curves were found to exhibit monoexponential relaxation behavior, indicating the presence of a single relaxing magnetization component. This conclusion was consistent with HSVD analysis which also indicated the presence of a single exponentially relaxing magnetization component in each data set.

NOE Measurements. $^{31}P\{^1H\}$ NOE values for phosphorus metabolites present in cortical and nuclear calf lens homogenates at 5 °C, respectively, were as follows: PME, 1.6, 1.6; P_i, 1.7, 1.7; GPC, 1.4, 1.3; α-ATP, 1.2; β-ATP, 1.0; γ-ATP, 1.5.

Aqueous BSA Solution. To experimentally assess the contribution of intermolecular relaxation effects to the measured $\tau_{0,eff}$ value, ^{31}P off-resonance rotating frame spin–lattice relaxation experiments were performed on mixtures of G-3-P (3.6 mM) and BSA (5.4 mM) prepared in ^2H_2O and H_2O (pH 6.8–6.9, 18 °C). $\tau_{0,eff}$ values of 16.9 ± 0.4 (intramolecular DD and CSA relaxation contributions assumed) and 13.3 ± 0.3 ns (intra- and intermolecular DD plus CSA relaxation contributions assumed) were obtained for G-3-P in ^2H_2O and H_2O, respectively. Correcting for the increased viscosity of ^2H_2O relative to H_2O [$\eta(^2H_2O)/\eta(H_2O) = 1.23$ at 25 °C, *Lange's Handbook of Chemistry* (Dean, 1985)] yielded a corrected $\tau_{0,eff}$ value of 13.7 ns for G-3-P in the presence of BSA dissolved in ^2H_2O. The excellent agreement between these $\tau_{0,eff}$ values determined in both "magnetic" and "nonmagnetic" solvents further supports the assumptions made about relaxation mechanism contributions to the off-resonance rotating frame spin–lattice relaxation experiment for the determination of phosphorus metabolite $\tau_{0,eff}$ values.

Similar experiments, in the presence and absence of 1 μM $MnCl_2$, performed on solutions of G-3-P (2.7 mM) and BSA (5.9 mM), pH 7.2 and 18 °C, yielded $\tau_{0,eff}$ values of 11.9 ± 0.3 and 11.7 ± 0.4 ns. Thus, no significant relaxation contribution effects from paramagnetic sources are indicated at metabolite and paramagnetic ion concentrations characteristic of those found in vertebrate lens tissue (Kuck, 1979; Harding & Crabbe, 1984).

Table V: Spin–Lattice Relaxation Times for Calf Lens Homogenate Phosphorus Metabolites at 5 °C

metabolite	T_1 (s) (cortical)	N^a	r^b	T_1 (s) (nuclear)	N^a	r^b
GPC	3.09 ± 0.05	31	0.9997	2.52 ± 0.03	31	0.9998
PME	4.45 ± 0.14	28	0.9990	3.88 ± 0.10	30	0.9990
P_i	5.28 ± 0.08	30	0.9998	3.96 ± 0.13	32	0.9984
α-ATP	0.93 ± 0.02	31	0.9979			
β-ATP	0.73 ± 0.07	31	0.9667			
γ-ATP	1.08 ± 0.03	31	0.9984			

[a] Number of data points. [b] Correlation coefficient.

Discussion

Quantitative analysis of the phosphorus metabolite spectral intensity ratio dispersion curves, R vs ω_e, assumed isotropic reorientational motion, intramolecular and intermolecular DD, and CSA relaxation mechanism contributions. The assumption of these mechanistic contributions in the analysis of the relaxation data is in agreement with ^{31}P NMR relaxation studies of 2,3-BPG in aqueous solution and in the intact erythrocyte, which indicate that DD (intra- and intermolecular) and CSA relaxation mechanisms are dominant (Christensen & Jacobsen, 1988). The excellent agreement obtained for the $\tau_{0,eff}$ values of G-3-P in concentrated mixtures of BSA prepared in H_2O and ^2H_2O using the relevant relaxation expressions (vide supra) in the data analysis furthermore supports the assumption of phosphorus relaxation mechanism contributions adopted in this study. The occurrence of a significant NOE for P_i is indicative of a DD relaxation contribution from solvent protons. Furthermore, two-dimensional heteronuclear NOE studies conducted in aqueous solution demonstrated the presence of different dipolar interaction strengths between solvent protons and the phosphorus nuclei of ATP (Yu & Levy, 1983). Two models for intermolecular relaxation may be considered for P_i: (i) solvent proton translational motion (see Theory) and (ii) a "structure-making" model incorporating tetrahedrally hydrogen-bonded water molecules of finite lifetime to P_i (McCain & Markley, 1980). Dipolar relaxation contributions from bound Mg^{2+} to phosphorus metabolites were ignored since T_1 and $T_{1\rho}^{off}$ calculations indicated a negligible contribution. The low paramagnetic ion content of lenticular tissue (Kuck, 1970; Harding & Crabbe, 1984) and the observation that physiological levels of Mn^{2+} do not affect $\tau_{0,eff}$ determinations allow a dismissal of paramagnetic ion relaxation contributions in the analysis.

The $\tau_{0,eff}$ values determined by the off-resonance rotating frame spin–lattice relaxation experiment are somewhat dependent on the choice of relaxation mechanisms and subsequent input parameters (e.g., CSA shielding tensor values) adopted in the analysis. As an example, the experimentally determined value of $\tau_{0,eff}$ for GPC at 10 °C (cortex) was 1.6 ns in both the presence and absence of an assumed intermolecular DD relaxation contribution (in addition to intramolecular DD and CSA relaxation contributions). However, for PME (cortex) the respective corresponding values were 4.2 and 4.4 ns; α-ATP, 11.2 and 12.2 ns; PME (nucleus) 14.2 and 17.2 ns. This behavior is consistent with the simulations shown in Figure 1A. A 50% decrease in δ_z, reflecting hypothetical alterations in the CSA shielding tensor of PME, reduces $\tau_{0,eff}$ for this metabolite in cortex from 4.4 to 4.2 ns. The other input parameters that enter into the least-squares analysis for obtaining $\tau_{0,eff}$ are reasonably well-defined [e.g., the lens water translational diffusion coefficient which was experimentally measured under the conditions employed in this study (Haner et al., 1989)]. Alternatively, to increase the estimated τ_{free} value of PME from 0.15 to 4.4 ns would require a 29-fold increase in the estimated value for the homogenate viscosity, or a 3.1-fold increase in the value of the hydrodynamic radius of this metabolite. Errors of this magnitude are extremely unlikely, and thus drastic changes in the input parameters would be required to achieve parity between the experimentally determined $\tau_{0,eff}$ value and the estimated value of τ_{free} obtained from the Stokes–Einstein equation for a given metabolite. Furthermore, if a "structure-making" model (McCain & Markley, 1980) is substituted for solvent translational motion to account for solvent proton DD relaxtion (a water residence time of 0.01 ns was assumed), the $\tau_{0,eff}$ values obtained for P_i in cortical and nuclear homogenates increased an average of 4 and 12%, respectively. Use of the KH_2PO_4 shielding tensor values in the analysis of the spectral intensity ratio dispersion data for P_i resulted in unacceptably large $\tau_{0,eff}$ values, and therefore, the shielding tensor values derived by ab initio quantum mechanical calculations were used. We note that McCain and Markley (1980) also used the theoretically derived shielding tensor values in their analysis of P_i relaxation in aqueous solution.

The off-resonance rotating frame spin–lattice relaxation experiments for lenticular phosphorus metabolites yield $\tau_{0,eff}$ values substantially different from one another and are significantly larger than expected for free, or unbound, metabolites in an environment equivalent in viscosity to cytoplasm. For the phosphorus metabolites present in cortical and nuclear homogenates (see Tables I and II) the same increasing trend in the values of $\tau_{0,eff}$ was observed: GPC < PME < $P_i \approx$ ATP. (ATP is not significantly present in nuclear homogenates.) For ATP slightly different values of $\tau_{0,eff}$, $R_{\omega=\infty}$, and Θ_{free} were obtained depending on whether the α-, β-, or γ-phosphorus resonances were employed. This observation suggests that the rigid *isotropic* model adopted for the rotational diffusion of phosphorus metabolites may be inadequate and that an anisotropic diffusion model may be more appropriate for ATP. The values of $\tau_{0,eff}$ for the metabolites present in nuclear homogenate are in each case longer than the corresponding value observed in the cortical homogenate, although for GPC the increase in $\tau_{0,eff}$ is significantly less.

Temperature-induced changes in metabolite $\tau_{0,eff}$ values that are contrary to what would be expected theoretically are consistent with the occurrence of a temperature-dependent partition between free and macromolecular bound metabolites. The partition between free and bound ligand is dependent upon the sign of the enthalpy change accompanying binding as well as on the dependence of lens protein conformation on temperature. Among the lens proteins γ-crystallin is known to undergo a phase transition at ca. 16 °C (Clark & Benedek, 1980). For example, the binding of L-α-glycerol phosphate to purified γ-crystallin has been shown to be greater at higher temperatures (Groth-Vassellii et al. 1988). Thus, the observed temperature dependence of $\tau_{0,eff}$ and Θ_{free} for PME in lens homogenates (both cortical and nuclear) is consistent with the binding behavior observed under in vitro conditions. However, to account for the analogous behavior of GPC (nuclear) the explanation is not clear. It may be related to the occurrence of the γ-crystallin phase transition accompanying cold cataract

formation in the nucleus (Clark & Benedek, 1980).

Physical characterization studies of purified calf lens proteins (Siezen et al., 1979; Andries et al., 1982; Bindels et al., 1983; Harding & Crabbe, 1984) indicate the following protein species in the cortex: α-crystallin, MW 780K, 40% of total soluble protein weight; β_H-crystallin, MW 100K–200K, 18% of total soluble protein; β_L-crystallin, MW 50K–80K, 27% of total soluble protein; LM- (β_S- and γ_H-) crystallin, MW 23K–28K, 6% of total soluble protein; γ_L-crystallin, MW 20K, 9% of total soluble protein. Nuclear lens proteins, by contrast, are somewhat larger: α-crystallin, MW 1100K, 35% of total soluble protein; β_H-crystallin, MW 110K–270K, 26% of total soluble protein, β_L-crystallin, MW 50K–80K, 11% of total soluble protein; LM- (β_S-) crystallin, MW 28K, 5% of total soluble protein; γ_L-crystallin, MW 20K, 23% of total soluble protein. Such studies fail to characterize the water-insoluble fraction, of which the major protein component is α-crystallin (Ortwerth & Olesen, 1988). Experimental determination of average $\tau_{0,eff}$ values for lens proteins of cortical and nuclear calf lens homogenates is consistent with the average values calculated using the known size distribution and composition of the water-soluble lens proteins (Morgan et al., 1989, 1990).

The phosphorus metabolite $^{31}P\{^1H\}$ NOE data indicate that a fraction of the metabolite population is engaged in fairly rapid reorientational motion. Taken together, the NOE and $\tau_{0,eff}$ data are consistent with the hypothesis that a fraction of certain phosphorus metabolites present in both bovine (calf) cortical and nuclear homogenates is noncovalently bound to a slowly tumbling macromolecular species, most likely to one or more members of the lens crystallin family. The detailed analysis of the heteronuclear NOE data in terms of an equilibrium between free and bound forms is in progress and will be reported elsewhere.

To evaluate the fractional extent of metabolite binding to a rigid isotropically reorienting macromolecule, a two-site fast-exchange model was assumed. The fast-exchange assumption (on the T_1 time scale) is supported by the observation of single-exponential inversion magnetization recovery in the calf lens cortical and nuclear homogenates. Furthermore, since nonexponential relaxation behavior was not observed, the influence of cross-relaxation as a contributing relaxation mechanism appears to be insignificant. In addition, the increase in T_1 values with B_0 field for PME and GPC and the field-independent ATP T_1 values (Williams et al., 1988) are consistent with fast exchange (on the T_1 time scale) between mobile and more slowly tumbling metabolites. The fast-exchange assumption was also employed by Moonen et al. (1986) in the analysis of kidney phosphorus metabolite T_1 relaxation data. The implicit assumptions inherent to this model are as follows: T_1, $T_{1\rho}^{eff}$, $T_2 \gg \tau_b$ and $\tau_b \gg \tau_{rot}$, where τ_b is the lifetime of the ligand in the bound state (chemical exchange correlation time) and τ_{rot} is the isotropic rotational correlation time of the macromolecule to which the ligand is bound. In addition, cross-relaxation between the phosphorus nuclei and protein nuclei in the protein-bound state was assumed to be negligible as noted above and as observed by Brauer and Sykes (1981) for phosphorus metabolite bound to protein.

Several complexities are inherent to this type of analysis. If $\tau_b \approx \tau_{rot}$, then the overall correlation time includes a contribution from τ_b [i.e., $\tau_0^{-1} = \tau_{rot}^{-1} + \tau_b^{-1}$ (Marshall, 1970)] and must be employed for the evaluation of the relevant relaxation times for ligand in the bound state. Another complication is that internal motional modes within the protein structure may affect the correlation time of the bound ligand (Marshall, 1970; Rose & Bryant, 1978), and thus the experimentally determined $\tau_{0,eff}$ value will not faithfully represent the contribution of metabolite bound to a reorienting macromolecule.

The lifetime of bound ions to proteins is not precisely known, but for Cl^- binding to HSA, τ_b has been estimated to be within the limits of 10^{-6}–10^{-8} s (Rose & Bryant, 1978). Since τ_{rot} values for proteins in lens tissue vary from ca. 20 to over 500 ns, the limit of very fast exchange would be expected to hold for ligand binding at the lower limit of the expected bound ion lifetime to all but the largest lens proteins. Spin–lattice relaxation times for phosphorus metabolites in calf lens homogenates are on the order of seconds, whereas the T_2 values are unknown. For other tissues such as heart, the T_2 of phosphorus metabolites is at least 20 ms (Turner & Garlick, 1984). Thus, the condition that τ_b is much less than the relaxation times appears to be a reasonable assumption. The question of how internal protein mobility affects τ_0 of the bound state is harder to judge. Brauer and Sykes (1981) observed the absence of protein internal mobility in the binding of ATP to a derivative of G-actin. Moreover, we noted for G-3-P binding to γ-crystallin that the binding site appears to be in the cleft formed by the two nearly homologous protein domains, which suggests a relatively rigid binding site (Groth-Vasselli et al., 1988).

Previous NMR studies from this laboratory (Morgan et al., 1989) demonstrated the presence of both solidlike and mobile protein domains in calf lens nuclear homogenates; cortical homogenates, by contrast, contained only a mobile protein fraction. Binding to solidlike protein structures would not be expected to yield NMR-"visible" signals because of the very broad line widths resulting from slow rotational motion; however, phosphorus metabolite exchange from these domains into the unliganded state or into a bound state which is tumbling more rapidly should be considered. The binding analysis should therefore take into account the possibility of binding to both mobile and solidlike protein species by incorporating chemical exchange mediated magnetization transfer of a phosphorus metabolite from a solidlike protein environment to the mobile protein domain. Phosphorus metabolites bound to solidlike protein domains would be NMR "invisible" in spectra obtained by use of the usual high-resolution NMR instrumentation and spectral acquisition conditions. For example, in liver ATP has been reported not to be 100% observable by ^{31}P NMR (Murphy et al., 1988) whereas ADP is usually NMR "invisible" in many tissues (Iles et al., 1985) including lens under many conditions (Greiner et al., 1981, 1982; Gonzalez et al., 1984; Willis & Schleich, 1986; Williams et al., 1988). Line width calculations for a phosphomonoester assuming intramolecular and intermolecular DD and CSA relaxation mechanism contributions indicate that a τ_0 value of 1 μs would result in a line width of ca. 200 Hz.

Off-resonance irradiation of broad resonances originating from very slowly tumbling phosphorus metabolites, such as those arising from binding to solidlike protein domains, is accomplished in the off-resonance rotating frame spin–lattice relaxation experiment and would result in saturation of the resonance. Use of this phenomenon enables the elimination of broad resonances with retention of narrow resonances representing "mobile" metabolites in ^{31}P in vivo MRS spectra of intact tissues as demonstrated by Ackerman et al. (1984) and Gonzalez-Mendez (1984). The finding that the limiting value of the fitted spectral intensity ratio is greater than 0.95 for most lenticular phosphorus metabolites indicates minimal contributions from chemical exchange effects originating from metabolite binding to solidlike protein domains. However, for PME present in both cortical and nuclear homogenates at 18 °C the limiting values of the spectral intensity ratio were found

to be less than 0.95. Quantitative analysis of these data indicates small, yet significant chemical exchange effects originating from NMR-"invisible" PME. The "detection" of exchange between "mobile" and "invisible" phosphorus metabolites illustrates further the utility of the off-resonance rotating frame spin–lattice relaxation experiment.

The control of metabolic activity has classically been assigned to enzyme concentration and activity. However, the realization that excess enzyme active site concentration rather than substrate concentrations controls the distribution of metabolites in the glycolytic pathway suggests that perhaps all of the metabolites except those of very high concentration are bound (Srivastava & Bernhard, 1986). Those metabolites present in a particular cell at high concentration probably represent the final product of an organized enzyme series. Such a metabolite would be expected to fluctuate under different physiological conditions and could serve as a ligand to enzymes or structural proteins, such as the lens crystallins, and thus act as a "signal" for the required response to a given stress. For example, in the lens of many species G-3-P and ATP are the most abundant phosphorus metabolites. In the calf lens (Pirie, 1962) the amount of G-3-P present in the cortex and nucleus is 0.590 and 0.253 mmol/kg of wet lens tissue, respectively. Lens protein composition and molecular weight data (vide supra) enabled the calculation of the γ-crystallin to G-3-P ratio. For the cortex, the most metabolically active region of the lens, this was found to be ca. 2.3, whereas for the more metabolically inactive nucleus the value increased to ca. 18.2. Thus, sufficient γ-crystallin for binding of these ligands appears to be present in both the lens cortex and nucleus.

The NMR-derived rotational diffusion results presented here suggest that certain cortical and nuclear lens phosphorus metabolites (PME, ATP, and P_i) bind to more slowly tumbling species, most likely lens structural proteins. By contrast, GPC was not bound to an appreciable extent. For PME, evidence for binding to solidlike protein domains was obtained in both cortical and nuclear homogenates at 18 °C. With the exception of P_i, the binding of PME and ATP to macromolecular species was found to be temperature dependent in the region of the cold cataract phase transition temperature. The significance of these findings for the control of lenticular metabolism and its relationship to transparency remain to be elucidated.

Acknowledgments

We thank Professor Glenn L. Millhauser for suggesting the use of HSVD analysis and for providing the necessary computer program. We gratefully acknowledge the help of Xiaowei Wang with the NOE experiments.

References

Abragam, A. (1961) *The Principles of Nuclear Magnetism*, pp 300–305, Oxford University Press, London.

Ackerman, J. J. H., Evelhoch, J. L., Berkowitz, B. A., Kichura, G. M., Duel, R. K., & Lown, K. S. (1984) *J. Magn. Reson. 56*, 318–322.

Andries, C., Backhovens, H., Clauwaert, J., de Block, J., de Voeght, F., & Dhont, C. (1982) *Exp. Eye Res. 34*, 239–255.

Barkhuijsen, H., de Beer, R., & van Ormondt, D. (1987) *J. Magn. Reson. 73*, 553–557.

Benesch, R., & Benesch, R. E. (1967) *Biochem. Biophys. Res. Commun. 26*, 162–167.

Bindels, J. G., Bessems, G. J. J., de Man, B. M., & Hoenders, H. J. (1983) *Comp. Biochem. Physiol. 76B*, 47–55.

Brauer, M., & Sykes, B. D. (1981) *Biochemistry 20*, 6767–6775.

Brauer, M., & Sykes, B. D. (1987) in *Phosphorus NMR in Biology* (Burt, C. T., Ed.) pp 153–184, CRC Press, Boca Raton, FL.

Cheng, H.-M., & Chylack, L. T., Jr. (1985) in *The Ocular Lens* (Maisel, H., Ed.) pp 223–264, Marcel Dekker, New York.

Christensen, M., & Jacobsen, J. P. (1988) *Magn. Reson. Med. 7*, 197–203.

Clark, J. I., & Benedek, G. B. (1980) *Biochem. Biophys. Res. Commun. 95*, 482–489.

Crouch, R., Hurlbert, S., & Ragouzeos, A. (1982) *J. Magn. Reson. 49*, 371–382.

Daniel, C., & Wood, F. S. (1980) *Fitting Equations to Data*, 2nd ed., Wiley, New York.

Dean, J. A., Ed. (1985) *Lange's Handbook of Chemistry* 13th ed., pp 10-99–10-100, McGraw-Hill, New York.

Farnsworth, P. N., Groth-Vasselli, B., Kuckel, C. L., & Macdonald, J. C. (1989) *Lens Eye Toxic. Res. 6*, 541–558.

Gerstein, B. C., & Dybowski, C. R. (1985) *Transient techniques in NMR of solids*, Academic Press, Orlando, FL.

Gonzalez, R. G., Barnett, P., Cheng, H.-M., & Chylack, L. T., Jr. (1984) *Exp. Eye Res. 39*, 553–562.

Gonzalez-Mendez, R., Litt, L., Koretsky, A. P., von Colditz, J., Weiner, M. W., & James, T. L. (1984) *J. Magn. Reson. 57*, 526–533.

Greiner, J. V., Kopp, S. J., Sanders, D. R., & Glonek, T. (1981) *Invest. Ophthalmol. Vis. Sci. 21*, 700–713.

Greiner, J. V., Kopp, S. J., Mercola, J. M., & Glonek, T. (1982) *Exp. Eye Res. 34*, 545–552.

Greiner, J. V., Kopp, S. J., & Glonek, T. (1985) *Invest. Ophthalmol. Vis. Sci. 26*, 537–544.

Groth-Vasselli, B., Schleich, T., & Farnsworth, P. N. (1988) *Invest. Ophthalmol. Vis. Sci. 29*, 186.

Haner, R. L., Schleich, T., Morgan, C. F., & Rydzewski, J. M. (1989) *Exp. Eye Res. 49*, 371–376.

Harding, J. J., & Crabbe, M. J. C. (1984) in *The Eye* (Davson, H., Ed.) 3rd ed., Vol. 1b, pp 244–492, Academic Press, London.

Hathaway, G. M., & Traugh, J. A. (1984) *J. Biol. Chem. 259*, 2850–2855.

Iles, R. A., Stevens, A. N., Griffiths, J. R., & Morris, P. G. (1985) *Biochem. J. 229*, 141–151.

James, T. L. (1984) in *Phosphorus-31 NMR* (Gorenstein, D. G., Ed.) pp 349–400, Academic Press, Orlando, FL.

James, T. L., Matson, G. B., & Kuntz, I. D. (1978) *J. Am. Chem. Soc. 100*, 3590–3594.

Kohler, S. J., & Klein, M. P. (1976) *Biochemistry 15*, 967–973.

Kuck, J. F. R., Jr. (1970) in *Biochemistry of the Eye* (Graymore, C. N., Ed.) pp 196–197, Academic Press, London.

Levy, G. C., & Peat, I. R. (1975) *J. Magn. Reson. 18*, 500–521.

Levy, R. M., Karplus, M., & McCammon, J. A. (1981) *J. Am. Chem. Soc. 103*, 994–996.

Marshall, A. G. (1970) *J. Chem. Phys. 52*, 2527–2534.

McCain, D. C. (1987) in *Phosphorus NMR in Biology* (Burt, C. T., Ed.) pp 25–61, CRC Press, Boca Raton, FL.

McCain, D. C., & Markley, J. L. (1980) *J. Am. Chem. Soc. 102*, 5559–5565.

McCain, D. C., & Markley, J. L. (1986) *J. Am. Chem. Soc. 108*, 4259–4264.

Moonen, C. T. W., Neal, L., & Cowgill, L. (1986) *Society*

of Magnetic Resonance in Medicine 5th Annual Meeting Abstracts (Works in Progress), pp 63-64.
Moonen, C. T. W., van Zijl, P. C. M., Le Bihan, D., & DesPres, D. (1990) Magn. Reson Med. 13, 467-477.
Morgan, C. F., Schleich, T., Caines, G. H., & Farnsworth, P. N. (1989) Biochemistry 28, 5065-5074.
Morgan, C. F., Schleich, T., & Caines, G. H. (1990) Biopolymers 29, 501-507.
Murphy, E., Gabel, S. A., Funk, A., & London, R. E. (1988) Biochemistry 27, 526-528.
Ortwerth, B. J., & Olesen, P. R. (1988) Exp. Eye Res. 48, 605-619.
Pirie, A. (1962) Exp. Eye Res. 1, 427-435.
Prado, F. R., Giessner-Prettre, C., Pullman, B., & Daudley, J.-P. (1978) J. Am. Chem. Soc. 101, 1737-1741.
Rose, K., & Bryant, R. G. (1978) J. Magn. Reson. 31, 41-47.
Schleich, T., Willis, J. A., & Matson, G. B. (1984) Exp. Eye Res. 39, 455-468.
Schleich, T., Matson, G. B., Willis, J. A., Acosta, G., Serdahl, C., Campbell, P., & Garwood, M. (1985) Exp. Eye Res. 40, 343-355.
Schleich, T., Morgan, C. F., & Caines, G. H. (1989a) Methods Enzymol. 176, 386-418.
Schleich, T., Caines, G. H., & Rydzewski, J. M. (1989b) Society of Magnetic Resonance in Medicine 8th Annual Meeting Abstracts (Works in Progress), p 1150.
Shriver, J. W., & Sykes, B. D. (1981) Biochemistry 20, 2004-2012.
Siezen, R., J., Bindels, J. G., & Hoenders, H. J. (1979) Exp. Eye Res. 28, 551-567.
Srivastava, D. K., & Bernhard, S. A. (1986) Science 234, 1081-1086.
Terao, T., & Hashi, T. (1974) J. Phys. Soc. Jpn. 36, 989-996.
Turner, C. J., & Garlick, P. B. (1984) J. Magn. Reson. 57, 221-227.
Williams, W. F., Austin, C. D., Farnsworth, P. N., Groth-Vasselli, B., Willis, J. A., & Schleich, T. (1988) Exp. Eye Res. 47, 97-112.
Willis, J. A., & Schleich, T. (1986) Exp. Eye Res. 43, 329-341.
Yoshizaki, K., Seo, Y., Nishikawa, H., & Morimoto, T. (1982) Biophys. J. 38, 209-211.
Yu, C., & Levy, G. C. (1983) J. Am. Chem. Soc. 105, 6994-6996.
Zigler, J. S., Jr., & Goosey, J. (1981) Trends Biochem. Sci. (Pers. Ed.) 6, 133-136.

Mutation of Essential Catalytic Residues in Pig Citrate Synthase†

Gerald M. Alter,‡ Joseph P. Casazza,§ Wang Zhi,‖ Peter Nemeth,‖ Paul A. Srere,‖ and Claudia T. Evans*,‖

Pre-Clinical Science Unit, Department of Veterans Affairs Medical Center, and Biochemistry Department, University of Texas Southwestern Medical Center, 4500 South Lancaster Road, Dallas, Texas 75216, Wright State University, Dayton, Ohio 45435, and NIAAA Laboratory of Metabolism and Molecular Biology, Rockville, Maryland

Received January 22, 1990; Revised Manuscript Received April 25, 1990

ABSTRACT: Two amino acid residues, His^{274} and Asp^{375}, were replaced singly in the active site of pig citrate synthase (PCS) with Gly^{274}, Arg^{274}, Gly^{375}, Asn^{375}, Glu^{375}, and Gln^{375}. The nonmutant protein and the mutant proteins were expressed in and purified from *Escherichia coli*, and the effects of these amino acid substitutions on the overall reaction rate and conformation of the PCS protein were studied by initial velocity and full time course kinetic analysis, behavior during affinity column chromatography, and monoclonal antibody reactivity. Native and mutant proteins purified similarly had a subunit molecular weight of 50 000 and were homologous when examined with 10 independent a-PCS monoclonal IgGs or with a polyclonal anti-PHCS serum. No activity was detected for Asn^{375} or Gln^{375}. The k_{cat}s of the other purified mutant proteins, however, were decreased by about 10^3 compared to the nonmutant enzyme activity. The K_m for oxalacetate was decreased 10-fold in the Glu^{375} protein and was reduced by half in Gly^{274} and Arg^{274} PCSs, while the K_m for acetyl-CoA was decreased 2-3-fold in Gly^{274}, Arg^{274}, and Gln^{375} PCSs. A mechanism is proposed that electrostatically links His^{274} and Asp^{375}.

The overall reaction catalyzed by citrate synthase (EC 4.1.3.7) is an aldol condensation reaction and is the first step of the Krebs tricarboxylic acid cycle (Wiegand & Remington, 1986; Srere, 1972). The reaction is stereospecific with respect to oxalacetate (OAA)[1] such that the acetyl group of acetyl coenzyme A adds to the si face of the keto moiety of oxalacetate with a concomitant inversion of the configuration of the methyl hydrogens (Eggerer et al., 1970; Retey & Arigoni, 1970). Three consecutive partial chemical reactions describe the course of catalysis by citrate synthase: enolization, condensation, and hydrolysis (Eggerer & Remberger, 1964; Buckel & Eggerer, 1969). The enzyme from pig heart is a dimeric protein of identical subunits whose X-ray crystal structure has been determined and whose mechanism has been intensively studied. The sequence of the enzyme from pig heart was derived from amino acid sequence analysis (Bloxham et al., 1981, 1982) and from the cDNA sequence (Evans et al.,

† This research was supported by grants from the Department of Veterans Affairs Medical Center, the U.S. Public Health Service, and the National Science Foundation.

* Address correspondence to this author of the Veterans Affairs Medical Center, 4500 S. Lancaster Rd., Dallas, TX 75216.
‡ Wright State University.
§ NIAAA Laboratory of Metabolism and Molecular Biology.
‖ University of Texas Southwestern Medical Center.

[1] Abbreviations: PCS, pig citrate synthase made by recombinant DNA methodology; PHCS, pig heart citrate synthase; His^{274}, Asp^{375}, PCS is the nonmutant pig citrate synthase from its unmodified cDNA expressed in and purified from *E. coli*; the mutant PCSs are designated by the residues substituted for His^{274}, or Asp^{375}; these are Gly^{274}, Arg^{274}, Gly^{375}, Asn^{375}, Glu^{375}, and Gln^{375}; SDS-PAGE, sodium dodecyl sulfate–polyacrylamide gel electrophoresis; acetyl-CoA, acetyl coenzyme A; OAA, oxalacetate.

0006-2960/90/0429-7557$02.50/0